

Kernel Learning for High-Resolution Time-Frequency Distribution

Lei Jiang, Haijian Zhang, Lei Yu, and Guang Hua

Abstract—The design of high-resolution and cross-term (CT) free time-frequency distributions (TFDs) has been an open problem. Classical kernel based methods are limited by the trade-off between TFD resolution and CT suppression, even under optimally derived parameters. To break the current limitation, we propose a data-driven kernel learning model directly based on Wigner-Ville distribution (WVD). The proposed kernel learning based TFD (KL-TFD) model includes several stacked multi-channel learning convolutional kernels. Specifically, a skipping operator is utilized to maintain correct information transmission, and a weighted block is employed to exploit spatial and channel dependencies. These two designs simultaneously achieve high TFD resolution and CT elimination. Numerical experiments on both synthetic and real-world data confirm the superiority of the proposed KL-TFD over traditional kernel function methods.

Index Terms—Kernel learning, kernel function, high-resolution time-frequency distribution.

I. INTRODUCTION

TIME-FREQUENCY distributions (TFDs) provide a comprehensive description of nonstationary signals [1]–[5], but their performances are restrained by issues such as time-frequency (TF) resolution, cross-terms (CTs), noise, spectrally overlapped components, etc. Therefore, high-resolution and CT-free TFDs [6], [7] to tackle the above issues are of vital importance for practical applications as most real-world signals are nonstationary and random [8]–[14].

Generally, linear TFDs suffer from low TF resolution, although some new linear TFDs have been explored [15]–[17]. Quadratic TFDs, e.g., Wigner-Ville distribution (WVD) [2], [18], have high TF resolution, but it is difficult for them to interpret the signal in 2-dimensional (2D) TF plane due to significant CTs [19]. Considerable investigations are therefore dedicated to reducing CTs while preserving high TF concentration. Particularly, kernel function based TFD methods viewed as smoothed versions of WVD have been studied [20], and they can be divided into two categories according to whether they depend on signals. Since CTs have oscillatory characteristics, signal-independent kernel functions are essentially low-pass filters, e.g., Choi-Williams distribution (CWD) [21] and B-distribution (BD) [22]. Moreover, the kernels separately smoothing along both time and frequency axes are designed to further improve TF resolution, e.g., S-method (SM) [23], extended modified B-distribution (EMBD) [24], and compact kernel distribution (CKD) [25].

However, the above signal-independent kernels require fixed or manually selected parameters, which might ignore some crucial information about signal’s intrinsic characteristics, e.g., the direction of analytic signals. Thus, signal-dependent kernels are designed with respect to certain criteria

to gain better TF representation, e.g., radially Gaussian kernel (RGK) [26], adaptive optimal-kernel (AOK) [27], [28], multi-directional distribution (MDD) [29], and adaptive directional TFD (ADTFD) [30]–[32]. Although most of signal-dependent kernels achieve better performance than signal-independent ones, they need to know the signal type and solve a kernel optimization problem subject to certain criteria. In addition, both signal independent and dependent kernel based methods have the limitation to simultaneously improve the performance of TF resolution and CT reduction. The above difficulties inspire us to develop new methods, aiming to break the trade-off between high TF resolution and negligible CTs.

Motivated by the 2D convolution relationship between WVD and smoothed TFDs, this letter proposes a kernel learning based TFD (KL-TFD) directly from WVD. We replace traditional kernel functions by designing a convolutional neural network (CNN), where multi-channel learning convolutional kernels are utilized to simulate traditional kernel functions.

II. THE PROPOSED KERNEL LEARNING BASED TFD

The architecture of the proposed KL-TFD model is shown in Fig. 1 (A), where a 2D Conv block is firstly used on signal’s WVD to obtain a multi-channel input. The KL-TFD mainly includes N stacked skipping weighted Conv modules, each of which consists of two 2D Conv blocks and one weighted block. The 2D Conv blocks with varying kernel sizes have the same structure, as shown in Fig. 1 (B). The weighted block is realized by the bottleneck attention module (BAM) [33], [34] to learn spatial and channel dependencies, as illustrated in Fig. 1 (C). Finally, a 2D Conv block and a 1×1 convolutional kernel convert multi-channel into single-channel output.

A. The KL-TFD Model

The ambiguity function (AF) of an analytic signal $z(t)$ is defined as:

$$A_z(\theta, \tau) = \int_{-\infty}^{\infty} z\left(t + \frac{\tau}{2}\right) z^*\left(t - \frac{\tau}{2}\right) e^{-j2\pi\theta t} dt, \quad (1)$$

where θ is the frequency shift, and τ is the time lag. Since Cohen’s class distributions can be interpreted as weighted versions of AF smoothed by a low-pass filter $\Phi(\theta, \tau)$, the general formula of Cohen’s class TFDs is expressed as [20]:

$$\zeta_z(t, f) = \int_{-\infty}^{\infty} \int_{-\infty}^{\infty} A_z(\theta, \tau) \Phi(\theta, \tau) e^{j2\pi(\theta t - f\tau)} d\theta d\tau. \quad (2)$$

When $\Phi(\theta, \tau) = 1$, $\zeta_z(t, f)$ is degenerated into WVD, which is the 2D Fourier transform of AF, i.e.,

$$W_z(t, f) = \int_{-\infty}^{\infty} z\left(t + \frac{\tau}{2}\right) z^*\left(t - \frac{\tau}{2}\right) e^{-j2\pi f\tau} d\tau. \quad (3)$$

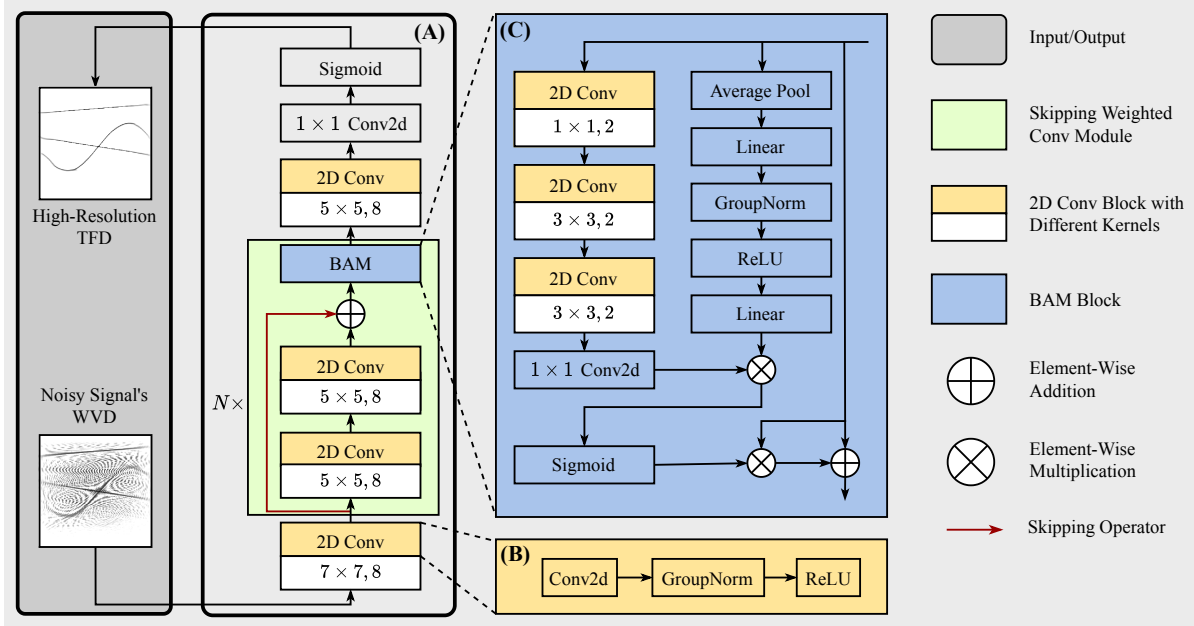


Fig. 1. Schematic diagram of the proposed kernel learning based TFD model. (A) The KL-TFD with N skipping weighted Conv modules, where the skipping operator is indicated by the red line. (B) The structure of the 2D Conv block. (C) The structure of the weighted block via BAM.

According to the convolution theorem and (3), the expression in equation (2) can be rewritten as the form of 2D convolution operation as below [20]:

$$\zeta_z(t, f) = W_z(t, f) ** \gamma(t, f), \quad (4)$$

where $**$ denotes the 2D convolution operator, and $\gamma(t, f)$ is a 2D convolutional kernel, which is computed by 2D Fourier transform of the AF kernel function $\Phi(\theta, \tau)$. Additionally, the ADTFD is defined as the 2D convolution of a quadratic TFD with an adaptive directional filter [31]:

$$\zeta_{\text{adapt}}(t, f) = W_z(t, f) ** \gamma_{\beta}(t, f), \quad (5)$$

where $\gamma_{\beta}(t, f)$ denotes the double derivative directional Gaussian filter, and β is the rotation angle with respect to the time axis. For each TF point, its angle is selected by solving an optimization problem over a group of directions [31].

Inspired by the 2D convolution relationship in (4) and (5), we propose to employ multi-channel learning convolutional kernels to replace kernel functions or adaptive directional filters. As seen in Fig. 1 (A), the signal's WVD serves as the input data, followed by N stacked skipping weighted Conv modules to obtain resolution improvement and CT elimination.

B. The 2D Conv Block Design with Skipping Operator

Each skipping weighted Conv module contains two 2D Conv blocks and a weighted block. Fig. 1 (B) shows the detail of a 2D Conv block, which involves a convolutional kernel followed by group normalization together with the ReLU function. It is examined that a larger kernel size leads to a more smooth TFD, we thus set the kernel sizes in the two 2D Conv blocks with 5×5 , and the number of filters are both set as $C = 8$. Since useful information may as well be transmitted with degradation in network, a skipping operator is used to maintain correct information transmission. Assuming

the number of frequency samples is equal to that of time samples. For a K -sample signal, given the output of the n -th skipping weighted Conv module $\zeta_{\text{sw}}^{(n)} \in \mathbb{R}^{C \times K \times K}$, we have the output of 2D Conv blocks after the n -th skipping operator:

$$\zeta_s^{(n)}(t, f) = \zeta_{\text{sw}}^{(n-1)}(t, f) ** \gamma_{s_{n_1}} ** \gamma_{s_{n_2}} + \zeta_{\text{sw}}^{(n-1)}(t, f), \quad (6)$$

where $n = 1, 2, \dots, N$ and $\zeta_{\text{sw}}^{(0)}(t, f)$ is the multi-channel WVD input (output of the 7×7 2D Conv block). $\gamma_{s_{n_1}}$ and $\gamma_{s_{n_2}}$ denote the kernels corresponding to the two 2D Conv blocks in the n -th skipping weighted Conv module.

C. The Weighted Block Design via BAM

To properly determine the direction of each TF point, element-wise weights are incorporated in a way such that primary directions are assigned with large weights, while insignificant directions are assigned with small ones. The directional filter in ADTFD adaptively selects directions by optimizing the correlation between the directional kernel and the modulus of TFD. In contrast, the data-driven kernel learning model can benefit from sufficient training data and our end-to-end network structure tends to be easy to train. To be specific, we adopt the same network architecture as the BAM [33] to utilize dependencies among TF coefficients as well as different channels, which is illustrated in Fig. 1 (C). Spatial dependencies can further distinguish auto-terms (ATs) from CTs as ATs and CTs have different directional features. Channel attention jointly attends to information from different representation subspaces. In order to reduce the amount of parameters, the 2D Conv blocks in BAM have smaller kernel sizes compared with those of skipping 2D Conv blocks. Channel and spatial weights are two separate branches, thus element-wise weights are computed as:

$$\omega_n = \sigma \left(\mathbf{F}_{ch}(\zeta_s^{(n)}) \otimes \mathbf{F}_{sp}(\zeta_s^{(n)}) \right), \quad (7)$$

where $n = 1, 2, \dots, N$ and $\omega_n \in \mathbb{R}^{C \times K \times K}$, \otimes denotes the element-wise multiplication. Channel weights are defined as:

$$\mathbf{F}_{ch}(\rho_n) = \sigma(g(\rho_n, \mathbf{W})) = \sigma(\mathbf{W}_2 \delta(\mathbf{W}_1 \rho_n)), \quad (8)$$

where $\mathbf{F}_{ch}(\rho_n) \in \mathbb{R}^{C \times K \times K}$, and $\rho_n \in \mathbb{R}^{C \times 1 \times 1}$ is the output of average pooling operator over $\zeta_s^{(n)}$. $g(x, \mathbf{W})$ represents a gating mechanism, which forms a bottleneck with two fully-connected layers around the non-linearity. The first fully-connected layer $\mathbf{W}_1 \in \mathbb{R}^{C \times C/r_c}$ achieves channel reduction with reduction ratio r_c , then non-linearity characteristic is introduced by δ (ReLU function), and the second fully-connected layer $\mathbf{W}_2 \in \mathbb{R}^{C/r_c \times C}$ increases the number of channels. Finally, channel weights are obtained by Sigmoid function $\sigma(x) = 1/(1 + \exp(-x))$. On the other hand, spatial weights are attained by a bottleneck module with four convolutional layers using a reduction ratio r_s :

$$\mathbf{F}_{sp}(\zeta_s^{(n)}) = \zeta_s^{(n)}(t, f) * \gamma_{w_{n1}} * \gamma_{w_{n2}} * \gamma_{w_{n3}} * \gamma_{w_{n4}}, \quad (9)$$

where $\mathbf{F}_{sp}(\zeta_s^{(n)}) \in \mathbb{R}^{C \times K \times K}$, and $\{\gamma_{w_{ni}}\}_{i=1,2,3,4}$ denote the kernels of the four Conv blocks in the n -th weighted block.

As a result, the weighted output in the n -th skipping weighted Conv module can be obtained via (6) to (9):

$$\zeta_{sw}^{(n)}(t, f) = \omega_n \otimes \zeta_s^{(n)}(t, f) + \zeta_s^{(n)}(t, f), \quad (10)$$

where $n = 1, 2, \dots, N$, and element-wise weights realize proper direction selection at each TF point. On the basis of the 2D Conv block with skipping operator, the BAM can attain channel and spatial dependencies as well, which further improves TF resolution and eliminates CTs.

From the viewpoint of parameter reduction, we make the choice of a 2D Conv block and a 1×1 convolutional kernel to conduct channel fusion on $\zeta_{sw}^{(N)} \in \mathbb{R}^{C \times K \times K}$ in (10), and the sum of all channels leads to a high-resolution and CT-free TFD, as illustrated in Fig. 1.

III. NUMERICAL EXPERIMENTS

The proposed KL-TFD model is compared with state-of-the-art kernel design methods [20], [32], including WVD [2], CKD [25], BD [22], EMBD [24], MDD [29], AOK [28], RGK [26], and ADTFD [30]. The ℓ_1 distance to model and Rényi entropy [10], [35] are regarded as two criteria to quantitatively assess the above-mentioned methods. For the parameter setting of the KL-TFD, channel reduction and spatial reduction in weighted blocks are set to $r_c = r_s = 4$. Our training dataset including 8×10^4 TF images is built by synthetic signal mixtures, each of which is constituted of two or three randomly spectrally-overlapped (only one intersection) linear frequency-modulated (LFM) and sinusoidal frequency-modulated (SFM) components with amplitude modulation (AM) at a fixed SNR = 10 dB. We train the KL-TFD network on the above training dataset using NVIDIA GeForce GTX 1080 GPUs with step decay learning rate schedule. Commonly-used binary cross entropy (BCE) loss function is adopted to obtain a robust network. Table I presents the ℓ_1 distance to model results on a three-component synthetic signal (shown in the second row of Fig. 2) at different SNR levels, implemented by our KL-TFD with varying number of the skipping weighted Conv modules,

TABLE I
 ℓ_1 DISTANCE TO MODEL USING OUR KL-TFD WITH INCREASING NUMBER OF THE SKIPPING WEIGHTED CONV MODULES.

SNR	$N = 3$	$N = 5$	$N = 7$	$N = 9$	$N = 11$	$N = 13$	$N = 15$
45 dB	1.60	1.53	1.22	1.19	1.15	1.15	1.13
35 dB	1.60	1.53	1.22	1.19	1.15	1.15	1.13
25 dB	1.61	1.53	1.22	1.19	1.15	1.15	1.14
15 dB	1.63	1.57	1.26	1.23	1.20	1.20	1.18
10 dB	1.69	1.63	1.33	1.32	1.29	1.28	1.28
5 dB	1.85	1.74	1.47	1.52	1.29	1.48	1.48
0 dB	2.27	1.87	1.72	1.98	1.46	1.81	1.82

i.e., $N \in \{3, 5, 7, 9, 11, 13, 15\}$. Note that the performance improves as the value of N increases when $\text{SNR} \geq 10$ dB, and becomes slightly inconsistent when $\text{SNR} < 10$ dB. The reason behind this issue is that we only train our model with data at $\text{SNR} = 10$ dB. To balance the performance and complexity in moderate-to-high SNR cases, we choose $\text{SNR} = 10$ dB for training and set $N = 9$ in the following experiments. One can build specific training data depending on practical requirements. For more information, please refer to <https://github.com/teki97/KL-TFD>.

A. TFDs of Synthetic Spectrally-Overlapped Signals

We consider a 256-sample two-component test signal containing an AM-LFM and an AM-SFM, as well as a 256-sample three-component test signal with two AM-LFM and an AM-SFM. The generated TFDs on these two synthetic signals using different TFD methods with $\text{SNR} = 10$ dB are shown in the first and second rows of Fig. 2. It is seen that the WVD is seriously disturbed by both CTs and noises. The CKD and EMBD suppress the noises at the sacrifice of TF resolution. Although the ADTFD can greatly eliminate CTs without TFD distortion by considering directions of TF points, it is crucial to make a balance between TF resolution and CT reduction. Besides, the parameters of filter shape and window length for the ADTFD are manually selected. Experimental results show that the proposed KL-TFD method can break the trade-off between high TF resolution and CT suppression, which is an issue often encountered by traditional TFDs.

TABLE II
 ℓ_1 DISTANCE TO MODEL USING DIFFERENT METHODS ON THE THREE-COMPONENT AM-FM SIGNAL AT VARIOUS SNR LEVELS.

SNR	WVD	EMBD	AOK	ADTFD	RGK	KL-TFD
45 dB	9.76	8.07	7.44	8.26	4.67	1.19
35 dB	9.77	8.08	7.43	8.27	4.67	1.19
25 dB	9.90	8.09	7.45	8.27	4.69	1.19
15 dB	10.75	8.40	7.61	8.34	4.87	1.23
5 dB	16.53	11.27	9.27	10.05	6.43	1.52
0 dB	25.22	17.61	13.37	14.64	10.16	1.98

To validate the noise robustness of different methods, the evaluation results measured by ℓ_1 distance to model on the three-component test signal are presented in Table II, where we change the SNR level of test data from 45 to 0 dB, and 100 trials are implemented at each SNR. Even though our training dataset only contains signals at $\text{SNR} = 10$ dB, the proposed KL-TFD always achieves a large performance gain compared

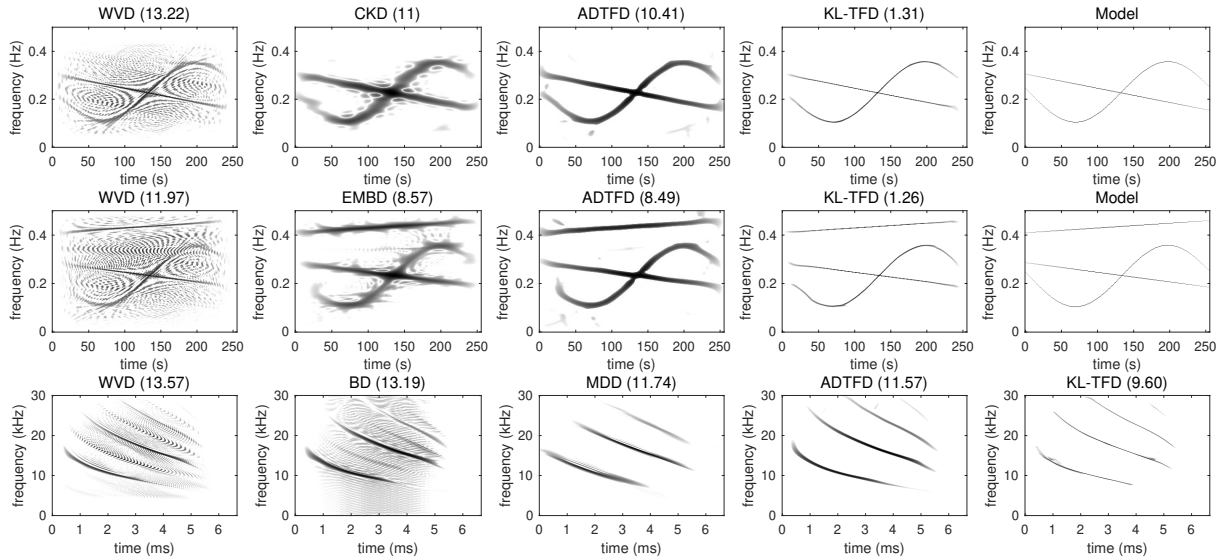


Fig. 2. Generated TFDs of synthetic and real-world data using WVD [2], BD [22], EMBD [24], MDD [29], CKD [25], ADTFD [30], and the proposed KL-TFD. **(First row)**: TFDs of a synthetic signal including an AM-LFM and an AM-SFM at SNR = 10 dB. The ℓ_1 distance to model is annotated on the top of each TFD. **(Second row)**: TFDs of a synthetic signal including two AM-LFM and an AM-SFM at SNR = 10 dB. The ℓ_1 distance to model is annotated on the top of each TFD. **(Last row)**: TFDs of a real-world bat echolocation signal. The Rényi entropy is annotated on the top of each TFD.

to other methods especially at low SNRs, which indicates that the kernel learning model is robust to noise.

B. TFDs of Real-World Signals

Although only trained on synthetic data, the proposed KL-TFD method is also validated over real-world data. We now examine the effectiveness of the KL-TFD method compared against WVD, BD, MDD, RGK, and ADTFD on a real-world bat echolocation signal with $K = 400$ samples [20], [36]. The visualized TFD results of the noiseless bat echolocation signal are shown in the last row of Fig. 2. It is observed that the signal-dependent methods achieve better performance than signal-independent WVD and BD, i.e., CTs are greatly removed. Moreover, only ADTFD and KL-TFD are capable of gaining the fourth part of the bat signal, whose energy is too low to recognize in most methods.

To independently assess the contribution of different parts in KL-TFD, we conduct a series of ablation experiments. The quantitative comparison results of different methods measured by Rényi entropy are presented in Fig. 3. Three observations can be made. First, the KL-TFD model without (w/o) the skipping operator and the weighted block when $N = 1$, i.e., only two 2D Conv blocks left in Fig. 1 (A), is trained and the test result is indicated with a blue curve in Fig. 3. Despite the simple network configuration, its performance is still superior over all the traditional kernel design methods, demonstrating the advantages and feasibility of data-driven kernel learning models. Second, the KL-TFD models without the skipping operator and/or the weighted block when $N = 9$ are implemented. Note from Fig. 3 that both of the skipping operator and the weighted block play important roles in improving performance, and the best result is achieved when we combine these two parts together. Third, it should be stressed that the trained KL-TFD model on synthetic signals is still effective

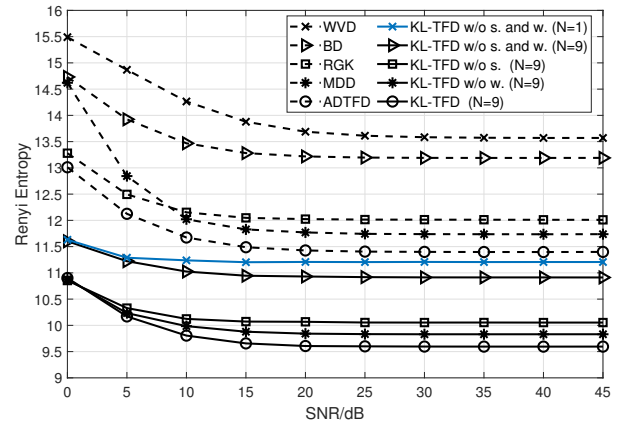


Fig. 3. Rényi entropy on real-world bat echolocation signal vs. SNR levels. (s. and w. denote the skipping operator and the weighted block, respectively)

for actual nonstationary bat signals, and can be generalized to test signals with more number of components. For other actual signals, e.g., EEG, the training dataset of the KL-TFD can be reconstructed to better learn EEG's characteristics.

IV. CONCLUSION

This letter attempts to generate high-resolution and CT-free TFDs by proposing a data-driven kernel learning model, which is designed as an end-to-end network to replace traditional kernel functions, where two skipping 2D Conv blocks and one weighted block are two dominant parts. Experimental results demonstrate that supervised kernel parameter learning methods using neural network based models for high-resolution TFDs outperform their traditional kernel design counterparts. Ablative analysis also examines the effectiveness of our proposed KL-TFD model. Future works may consider the signal TF analysis with missing data [37]–[39].

REFERENCES

- [1] L. Stankovic, M. Dakovic, and T. Thayaparan, "Time-Frequency Signal Analysis With Applications," *Artech House*, 2013.
- [2] B. Boashash, "Time-Frequency Signal Analysis and Processing (Second Edition)," *Academic Press*, 2016.
- [3] P. Flandrin, "Explorations in Time-Frequency Analysis," *Cambridge University Press*, 2018.
- [4] N. Saulig, J. Lerga, Ž. Milanović, and C. Ioana, "Extraction of Useful Information Content From Noisy Signals Based on Structural Affinity of Clustered TFDs' Coefficients," *IEEE Trans. Signal Process.*, vol. 67, no. 12, pp. 3154–3167, Jun. 2019.
- [5] H. Zhang, G. Hua, and Y. Xiang, "Enhanced Time-Frequency Representation and Mode Decomposition," *IEEE Trans. Signal Process.*, pp. 1–1, 2021.
- [6] L. Zuo, M. Li, Z. Liu, and L. Ma, "A High-Resolution Time-Frequency Rate Representation and the Cross-Term Suppression," *IEEE Trans. Signal Process.*, vol. 64, no. 10, pp. 2463–2474, 2016.
- [7] L. Zuo, M. Li, and X. Xia, "New Smoothed Time-Frequency Rate Representations for Suppressing Cross Terms," *IEEE Trans. Signal Process.*, vol. 65, no. 3, pp. 733–747, 2017.
- [8] V. S. Amin, Y. D. Zhang, and B. Himed, "Improved Time-Frequency Representation of Multi-Component FM Signals with Compressed Observations," in *54th Asilomar Conference on Signals, Systems, and Computers*, 2020, pp. 1370–1374.
- [9] S. Zhang and Y. D. Zhang, "Low-rank hankel matrix completion for robust time-frequency analysis," *IEEE Trans. Signal Process.*, vol. 68, pp. 6171–6186, 2020.
- [10] P. Flandrin and P. Borgnat, "Time-Frequency Energy Distributions Meet Compressed Sensing," *IEEE Trans. Signal Process.*, vol. 58, no. 6, pp. 2974–2982, Jun. 2010.
- [11] H. Zhang, G. Bi, W. Yang, S. G. Razul, and C. M. S. See, "IF estimation of FM signals based on time-frequency image," *IEEE Transactions on Aerospace and Electronic Systems*, vol. 51, no. 1, pp. 326–343, 2015.
- [12] H. Zhang, G. Bi, S. G. Razul, and C. M. S. See, "Robust time-varying filtering and separation of some nonstationary signals in low SNR environments," *Signal Processing*, vol. 106, pp. 141–158, 2015.
- [13] E. Sejdíć, I. Djurović, and J. Jiang, "Time-frequency feature representation using energy concentration: An overview of recent advances," *Digital Signal Processing*, vol. 19, no. 1, pp. 153–183, 2009.
- [14] I. Volaric, V. Sucic, and S. Stankovic, "A Data Driven Compressive Sensing Approach for Time-Frequency Signal Enhancement," *Signal Process.*, vol. 141, pp. 229–239, Dec. 2017.
- [15] G. Yu, M. Yu, and C. Xu, "Synchroextracting Transform," *IEEE Trans. Ind. Electron.*, vol. 64, no. 10, pp. 8042–8054, 2017.
- [16] G. Yu, Z. Wang, and P. Zhao, "Multisynchrosqueezing Transform," *IEEE Trans. Ind. Electron.*, vol. 66, no. 7, pp. 5441–5455, 2019.
- [17] Y. Abdoush, G. Pojani, and G. E. Corazza, "Adaptive Instantaneous Frequency Estimation of Multicomponent Signals Based on Linear Time-Frequency Transforms," *IEEE Trans. Signal Process.*, vol. 67, no. 12, pp. 3100–3112, 2019.
- [18] M. F. Al-Sa'd, B. Boashash, and M. Gabbouj, "Design of an Optimal Piece-Wise Spline Wigner-Ville Distribution for TFD Performance Evaluation and Comparison," *IEEE Trans. Signal Process.*, pp. 1–1, 2021.
- [19] F. Hlawatsch and G. F. Boudreaux-Bartels, "Linear and quadratic time-frequency signal representations," *IEEE Signal Processing Magazine*, vol. 9, no. 2, pp. 21–67, 1992.
- [20] B. Boashash and S. Ouelha, "Designing high-resolution time-frequency and time-scale distributions for the analysis and classification of nonstationary signals: a tutorial review with a comparison of features performance," *Digital Signal Processing*, vol. 77, pp. 120 – 152, 2018.
- [21] H. I. Choi and W. J. Williams, "Improved Time-Frequency Representation of Multicomponent Signals Using Exponential Kernels," *IEEE Transactions on Acoustics, Speech, and Signal Processing*, vol. 37, no. 6, pp. 862–871, Jun. 1989.
- [22] B. Barkat and B. Boashash, "A High-Resolution Quadratic Time-Frequency Distribution for Multicomponent Signals Analysis," *IEEE Trans. Signal Process.*, vol. 49, no. 10, pp. 2232–2239, Oct. 2001.
- [23] L. Stankovic, "A Method for Time-Frequency Analysis," *IEEE Trans. Signal Process.*, vol. 42, no. 1, pp. 225–229, Jan. 1994.
- [24] B. Boashash, G. Azemi, and J. M. O'Toole, "Time-Frequency Processing of Nonstationary Signals: Advanced TFD Design to Aid Diagnosis with Highlights From Medical Applications," *IEEE Signal Process. Mag.*, vol. 30, no. 6, pp. 108–119, Nov. 2013.
- [25] M. Abed, A. Belouchrani, M. Cheriet, and B. Boashash, "Time-frequency distributions based on compact support kernels: Properties and performance evaluation," *IEEE Transactions on Signal Processing*, vol. 60, no. 6, pp. 2814–2827, 2012.
- [26] R. G. Baraniuk and D. L. Jones, "Signal-dependent Time-Frequency Analysis Using a Radially Gaussian Kernel," *Signal Process.*, vol. 32, no. 3, pp. 263–284, Jun. 1993.
- [27] D. L. Jones and R. G. Baraniuk, "An Adaptive Optimal-Kernel Time-Frequency Representation," in *Int. Conf. Digital Signal Process.*, vol. 4, USA, 1993, pp. 109–112.
- [28] D. L. Jones and R. G. Baraniuk, "An adaptive optimal-kernel time-frequency representation," *IEEE Trans. Signal Process.*, vol. 43, no. 10, pp. 2361–2371, 1995.
- [29] B. Boashash and S. Ouelha, "An Improved Design of High-Resolution Quadratic Time-Frequency Distributions for the Analysis of Nonstationary Multicomponent Signals Using Directional Compact Kernels," *IEEE Trans. Signal Process.*, vol. 65, no. 10, pp. 2701–2713, May 2017.
- [30] N. A. Khan and B. Boashash, "Multi-Component Instantaneous Frequency Estimation Using Locally Adaptive Directional Time Frequency Distributions," *International Journal of Adaptive Control and Signal Processing*, vol. 30, no. 3, pp. 429–442, 2016.
- [31] N. Ali Khan and S. Ali, "Sparsity-aware adaptive directional time-frequency distribution for source localization," *Circuits Syst. Signal Process.*, vol. 37, no. 3, p. 1223–1242, Mar. 2018.
- [32] M. Mohammadi, A. A. Pouyan, N. A. Khan, and et al., "Locally Optimized Adaptive Directional Time-Frequency Distributions," *Circuits, Systems, and Signal Processing*, vol. 37, no. 8, pp. 3154–3174, 2018.
- [33] J. Park, S. Woo, J.-Y. Lee, and I. S. Kweon, "BAM: bottleneck attention module," *CoRR*, vol. abs/1807.06514, 2018.
- [34] —, "A Simple and Light-Weight Attention Module for Convolutional Neural Networks," *Int J Comput Vis*, vol. 128, p. 783–798, 2020.
- [35] L. Stanković, "A measure of some time-frequency distributions concentration," *Signal Process.*, vol. 81, no. 3, pp. 621–631, 2001.
- [36] B. Boashash and S. Ouelha, "Efficient software platform TFSAP 7.1 and Matlab package to compute Time-Frequency Distributions and related Time-Scale methods with extraction of signal characteristics," *SoftwareX*, vol. 8, pp. 48–52, 2018.
- [37] V. S. Amin, Y. D. Zhang, and B. Himed, "Sparsity-based Time-Frequency Representation of FM Signals With Burst Missing Samples," *Signal Process.*, vol. 155, pp. 25–43, Feb. 2019.
- [38] S. Zhang and Y. D. Zhang, "Robust Time-Frequency Analysis of Multiple FM Signals With Burst Missing Samples," *IEEE Signal Process. Lett.*, vol. 26, no. 8, pp. 1172–1176, 2019.
- [39] N. A. Khan, M. Mohammadi, and I. Stankovic, "Sparse reconstruction based on iterative TF domain filtering and Viterbi based IF estimation algorithm," *Signal Process.*, vol. 166, p. 107260, 2020.